Sustainable Food Technology

ROYAL SOCIETY OF CHEMISTRY

PAPER

View Article Online
View Journal

Cite this: DOI: 10.1039/d6fb00088f

Antioxidant blend films of PLA and PVA with almond skin powder to preserve toasted almonds

Irene Gil-Guillén, * Chelo González-Martínez and Amparo Chiralt

The development of sustainable food packaging that minimizes the environmental impact of plastics, making use of natural resources, is necessary. In this regard, mixed PLA and PVA (75 : 25) films with and without almond skin powder have been studied for their ability to prevent the oxidation of roasted almonds during storage. PLA was dispersed homogeneously in the PVA matrix with good interfacial adhesion, modifying the crystallization of PVA. PLA reduced the water vapour permeability (WVP) of PVA by 50%, while increasing the oxygen permeability (OP) (56%) in the blend films. However, the incorporation of AS powder reduced OP values of blend films below that of neat PVA, without a significant increase in WVP. AS powder promoted the stiffness of the blend films (by 233%) reducing their extensibility (by 50%), but without significant effect on the resistance to break. Likewise, the PLA/PVA-AS films reduced the oxidation rate of packaged toast almonds during storage at 25 °C and 53% RH for 6 months, in comparison with the control films. Therefore, PVA/PLA-AS films represent a sustainable alternative for packaging low moisture foods sensitive to oxidation, while contributing to valorisation of a highly produced agri-food waste.

Received 24th March 2026
Accepted 6th May 2026

DOI: 10.1039/d6fb00088f

rsc.li/susfoodtech

Sustainability spotlight

This study represents a breakthrough in the field of sustainable food packaging through the development of biodegradable PVA/PLA composite films incorporating almond skin (AS). By repurposing almond skin powder, a very common agri-food waste product, this study has developed an eco-friendly material that significantly reduces the oxidation rate of roasted almonds, thereby extending the shelf life of sensitive foods. This research aligns directly with SDG 12 (Responsible Consumption and Production) by integrating agricultural by-products into a circular economy framework. Furthermore, it supports SDG 2 (Zero Hunger) by minimising post-harvest food losses, thanks to improved barrier properties. By offering a biodegradable alternative to conventional plastics, this work aims to diminish environmental impact and promotes sustainable industrial innovation.

1 Introduction

Plastics have become essential materials in both industrial production and everyday life due to their high strength, low weight, chemical stability and low manufacturing cost. However, their high chemical stability also poses serious environmental challenges due to their low degradation rate, making them persistent pollutants that threaten ecosystems.[1,2] During their prolonged degradation process, they gradually fragment, generating microplastics.[3] The most effective way to reduce their environmental pollution is to significantly reduce their use.[4,5] However, this approach is unrealistic, given the essential role that plastics play in the global economy. Therefore, other practices, such as recovery and recycling, are necessary to ensure the proper disposal and responsible management of plastic waste. Another alternative is the use of biodegradable plastics, which offer a more sustainable option compared to conventional plastics.[6]

Nowadays, manufacturers are responding to growing environmental awareness, driving the increased use of recycled materials and a significant demand for biopolymers to replace non-degradable plastics in sectors such as agriculture, food industry, and biomedicine.[7,8] The primary application of biodegradable polymers is packaging, including both flexible and rigid forms, with the most commercialized products being garbage bags, flexible and rigid containers, and disposable tableware.[9,10] Biodegradable plastics are defined as materials that maintain their functional properties throughout their intended use, yet can break down under natural environmental conditions into non-harmful substances that can be reintegrated into the organic matter cycle.[10,11] Bioplastics refer to polymers that are biodegradable, bio-based, or both. However, the term can be misleading, as bio-based plastics are not necessarily biodegradable.[8] Biodegradable plastics can include materials synthesized from bio-based monomers, such as PLA, as well as certain fossil-derived polymers that also undergo biodegradation, such as PVA.[10]

Instituto Universitario de Ingeniería de Alimentos para El Desarrollo, Universitat Politècnica de València, Camí de Vera s/n, 46022 València, Spain. E-mail: igilgui@upv.es

Polylactic acid (PLA), a linear aliphatic thermoplastic polyester derived from lactic acid, is the most produced bio-based and biodegradable polymer.[12] PLA is produced from renewable resources such as corn, wheat, or rice, thereby reducing reliance on fossil fuels. Additionally, it is biodegradable, recyclable, and compostable, making it a sustainable alternative to conventional plastics.[13,14] Nevertheless, it presents limitations, including significant brittleness with elongation at break below 10%, low oxygen barrier capacity, and a relatively slow degradation rate, which is influenced by crystallinity, molecular weight, morphology, water diffusivity, and the presence of stereoisomers.[14] Within the biodegradable polymers, polyvinyl alcohol (PVA) is a synthetic polymer derived from fossil resources that is water soluble and biocompatible. It has attracted attention in food packaging due to its flexibility, transparency, mechanical strength, and non-toxicity, with its primary application being the production of water-soluble films.[15,16] It has a high oxygen barrier capacity, which is advantageous in preventing the oxidation of sensitive foods, such as those containing unsaturated fats. However, its high hydrophilicity gives it very little water vapor barrier capacity, which is a problem for packaging moist foods.

The incorporation of PLA into PVA matrices has been shown to reduce their hydrophilicity, significantly increasing the water contact angle. PVA/PLA blends with up to 15% PLA[17] demonstrated the formation of hydrogen bonds between both polymers, which improved their compatibility and allowed uniform dispersion of PLA in the PVA matrix in the form of small spheres. This improved the processability by decreasing the melting viscosity, as well as the crystallinity, mechanical properties, and water resistance of the blends. Wang *et al.*[18] also analysed polymer interactions in PVA/PLA blends and observed a significant effect of PLA on hydrogen bonds between PVA chains, while improved mechanical performance of the blends compared to PVA up to a PVA : PLA ratio of 70 : 30. Likewise, Fan *et al.*[19] also used PLA to improve the hydrophobicity of PVA in order to obtain an effective packaging material to indicate the quality of shiitake mushrooms.

Several studies have proposed the incorporation of fibres derived from agri-food residues as reinforcing agents in polymers, enhancing the properties of conventional polymers and improving their suitability for industrial applications.[20,21] The almond skin is a lignocellulosic matrix that forms the outer protective layer of the almond fruit, is brown in colour and acts as a barrier to oxidation and microbial contamination of the seed.[22,23] The primary constituents of the almond skin are cellulose, hemicellulose, and lignin, with reported contents ranging from 20 to 38%, 8 to 28%, and 20 to 50%, respectively.[23] In addition, almond skin is rich in bioactive compounds, including flavonoids (*e.g.*, catechin), phenolic acids (hydroxybenzoic, hydroxycinnamic, and caffeic acids), proanthocyanidins, and triterpenoids (betulinic, ursolic, and oleanolic acids), as well as flavonol and phenolic glycosides, exhibiting notable antioxidant and antimicrobial activities.[22,24] Consequently, its incorporation into food packaging design is of considerable interest for developing reinforced and active materials capable of extending the shelf life of food products.[24,25]

Previous studies on PLA and PVA composites with almond skin powder revealed that the filler provided the films of both polymeric matrices with a strong UV light-blocking effect, antioxidant properties and improved oxygen barrier capacity.[24] Nevertheless, individual polymers have high permeability to oxygen (PLA) or water vapour (PVA) to adequately preserve certain food products, such as toast almonds, during storage. Blended PLA and PVA films could allow the barrier properties of the packaging materials to be modulated, making them more suitable for meeting food packaging requirements, while the almond skin would provide the films with antioxidant properties.

The aim of this study was to produce biodegradable packaging materials from PVA/PLA blends with improved suitability for packaging certain foods, while at the same time recovering high-volume agri-food waste, such as almond skins from industrial almond peeling. This could potentially reduce material costs and improve the protective performance of films for foods prone to oxidation. To this end, 15% by weight of almond skin powder was incorporated into PLA/PVA (75 : 25) blend films, and its effect on the polymer properties, mechanical and barrier performance of materials, and protective effect on packaged roasted almonds was analysed. Mono-polymer films with and without almond skin powder were also studied for comparison purposes and to better understand its effects on blend films.

2 Materials and methods

2.1 Materials

Almond skin (AS) (Prunus dulcis, var. Nonpareil de California) was kindly provided by Importaco S.A. (Valencia, Spain). PLA 4043D was supplied by NatureWorks (Plymouth, MN, USA), with a molecular weight of 111 kDa. Polyvinyl alcohol (PVA) with a molecular weight of 30–70 kDa and a hydrolysis degree of 87–90% was obtained from Sigma-Aldrich (Steinheim, Germany). The reagents P_2O_5, magnesium nitrate, isooctane, glacial acetic acid, potassium hydroxide, 1-decanol, potassium iodide, ethanol and potassium permanganate pentahydrate were also supplied by Sigma-Aldrich (Steinheim, Germany). Diethyl ether and phenolphthalein indicator were supplied by Panreac (Barcelona, Spain). Almonds (Marcona variety) for the packaging study were purchased at the central market (Valencia, Spain).

2.2 Raw material preparation

The almond skins were dried at 40 ± 2 °C for 3 days in a forced-air oven (SP Selecta, SA, Barcelona, Spain). The dried almond skins were then ground using a stainless-steel mill, IKA (SM300, Retsch GmbH, Haan, Germany), and sieved to obtain particles smaller than 63 μm, which were stored at 0% relative humidity until use. Due to their high oil content, the dried material was defatted by Soxhlet extraction with petroleum ether (40–60 °C). Almond oil was recovered using a vacuum rotary evaporator (Heidolph Instruments GmbH & Co. KG, Walpersdorfer, Germany) at 35 °C.

The defatted almond skin powder (AS) was stored at 0% relative humidity (HR) (in a desiccator with P_2O_5) to avoid moistening. The AS powder contained 13% protein, 10% cellulose, 12% hemicellulose, 17% lignin, and about 3% total phenol content, as reported in a previous study by Freitas *et al.*,[23] and exhibited DPPH radical scavenging capacity (5 mg mg^{-1} DPPH).[24]

2.3 Obtaining the films

PLA, PVA, and AS powder were dried at 60 °C in a vacuum oven and melt blended using an internal mixer (HAAKETM PolyLabTM QC, Thermo Fisher Scientific, Karlsruhe, Germany) according to the mass fraction shown in Table 1 for each film formulation. For formulations including PVA, this was previously plasticised in the internal mixer with 10% glycerol. In films containing AS, 15% of the powder was incorporated into the blend. The resulting mixtures were cryo-milled with liquid N_2 to obtain fine powders, which were then thermoformed into films (4 g per film) using a hydraulic press (LP20, Labtech Engineering, Thailand).

For PLA films, melt-blending was carried out at 160 °C, 50 rpm, for 6 min and film thermo-formation was performed by applying 3 min preheating at 160 °C, 3 min pressing at 100 bar, and 3 min cooling to 80 °C. For PVA films, melt blending and compression moulding were carried under the same conditions but at 180 °C. For PVA/PLA blend films, a 75 : 25 ratio of pre-compounded PVA–glycerol and PLA were melt blended at 180 °C, for 10 min, at 150 rpm, to favour the homogenisation of the blend. The film thermoforming was carried out applying the same conditions used for PVA films.

2.4 Characterisation of the films

2.4.1 Microstructure. Cross-sectional images of the films were obtained by field-emission scanning electron microscopy (FESEM) using a ZEISS® GeminiSEM 500 (Oxford Instruments, Oxford, UK). Samples were conditioned over P_2O_5 for 48 h, cryofractured in slush nitrogen, and mounted. Samples were sputter-coated with platinum and examined at an accelerating voltage of 2 kV.

2.4.2 Thermal properties. Film samples equilibrated at 0% relative humidity to avoid water interferences were analysed for phase transitions by Differential Scanning Calorimetry (DSC) and thermal stability by Thermogravimetric Analysis (TGA). DSC was performed using a STARe system (Mettler-Toledo Inc., Greifensee, Switzerland). Film samples (3–5 mg) were placed in aluminium pans and subjected to sequential heating, cooling and reheating under nitrogen flow (30 mL min^{-1}), with an empty pan as a reference. Films containing PVA were heated from 20 to 210 °C at 10 °C min^{-1}, held for 1 min, cooled to 20 °C at 10 °C min^{-1}, held for 1 min and reheated to 210 °C at 10 °C min^{-1}. PLA samples were similarly analysed from 25 to 160 °C. All measurements were performed in duplicate. The glass transition temperature (T_g), melting temperature (T_m) and melting enthalpy (ΔH_m) were determined from the second heating, while the crystallisation temperature (T_c) was obtained from the cooling scan.

Thermogravimetric analysis was performed with a TGA 1 STARe System (Mettler-Toledo Inc., Greifensee, Switzerland). Approximately 3–5 mg of sample was placed in an alumina crucible and heated from 25 to 600 °C at 10 °C min^{-1} under a nitrogen flow of 10 mL min^{-1}. DTGA curves were obtained with the STARe software (v12.00a) to determine the temperature corresponding to the maximum degradation rate for each mass-loss event. All measurements were conducted in duplicate.

2.4.3 Fourier transform infrared (FTIR) spectra. IR spectra of the films conditioned at a relative humidity of 53% were obtained in duplicate using an Agilent Cary 630 FTIR spectrometer fitted with an attenuated total reflectance (ATR) accessory. Measurements were taken in the range of 4000 to 650 cm^{-1} with a resolution of 6 cm^{-1}, averaging 128 sweeps per spectrum.

2.4.4 Oxygen and water vapour barrier properties. Water vapour permeability (WVP) of the films was measured gravimetrically following ASTM E96/E96M,[26] with modifications adapted from McHugh *et al.*[27] Circular film samples conditioned at 53% RH were sealed over Payne permeability cups (Elcometer SPRL, Hermelle/Argenteau, Belgium) containing 5 mL of distilled water (100% RH). The cups were placed in desiccators at 25 °C and 53% RH and maintained with an oversaturated $Mg(NO_3)_2$ solution, establishing a constant 100–53% RH gradient across the films. Weight measurements were taken every 75 min for 27 h using an analytical balance (ME36S, Sartorius, ±0.0001 g). WVP was calculated from the weight loss *versus* time slope in a steady-state, considering the film thickness measured with a digital micrometre (Comecta S.A., Barcelona) and the vapour pressure gradient across the film. All measurements were performed in triplicate.

Oxygen permeability (OP) of the films conditioned at 53% RH was measured using a Systech Illinois Model 8101e (Illinois, USA) following ASTM D3985-05.[28] The oxygen transmission rate of 50 cm^2 samples was recorded every 15 min until equilibrium was reached. Film thickness was measured with a digital micrometre (Palmer, Comecta, Barcelona, Spain), and the OP was calculated as the product of film thickness and transmission rate divided by the oxygen partial pressure gradient. Measurements were performed in triplicate for each formulation.

2.4.5 Optical properties. The reflectance spectra (400–700 nm) of the films conditioned at 53% RH were recorded using a spectrocolorimeter (CM-3600d, Minolta Co., Tokyo, Japan) over white (R) and black (R_0) backgrounds with known reflectance (R_g). Using the Kubelka–Munk multiple-scattering model,

Table 1 Mass fraction (g g^{-1}) of different components in different film formulations

Sample	PLA	PVA	Gly	AS
PLA	1.000	0.000	0.000	0.000
PLA-AS	0.850	0.000	0.000	0.150
PVA	0.000	0.900	0.100	0.000
PVA-AS	0.000	0.765	0.085	0.150
PVA/PLA	0.250	0.675	0.075	0.000
PVA/PLA-AS	0.226	0.578	0.058	0.150

the infinite-thickness reflectance (R_∞) was calculated (eqn (1)–(3)). CIE Lab* coordinates were derived from R_∞ using illuminant D65, and a 10° observer was determined.

$$R_\infty = a - b \tag{1}$$

$$a = \frac{1}{2}\left[R + \left(\frac{R_0 - R + R_g}{R_0 \cdot R_g}\right)\right] \tag{2}$$

$$b = \sqrt{a^2 - 1} \tag{3}$$

The UV-visible transmission spectra of the films were also measured, using a spectrophotometer (Evolution 201, Thermo Scientific, USA) from 200 to 800 nm. Each film formulation was analysed in duplicate.

2.4.6 Mechanical properties. Tensile force–deformation curves of films conditioned at 53% RH were obtained using a universal testing machine (TA.XTplus, Stable Micro Systems, Haslemere, UK) following ASTM D882.[29] From the resulting plots, the elastic modulus (EM), tensile strength (TS), and strain at break (E%) were determined. Film strips (25 × 100 mm) were tested with a 50 mm length at 50 mm min^{-1}. Five films were evaluated per formulation.

2.5 Antioxidant capacity of the films in packaged toasted almonds

The ability of the blend films, with and without AS powder, to preserve the quality of roasted almonds stored at 25 °C and 53% relative humidity was evaluated. The almonds were previously roasted in an oven (SP Selecta, SA, Barcelona, Spain) at 152 °C for 15 min, as described by ref. 30 for dark roast. The final moisture content of the roasted almonds was 3.1% (db), with a corresponding a_w value of 0.53. Heat-sealed bags (7.5 × 10 cm) were prepared from PLA–PVA blended films, with and without almond skin powder, and used to package the almonds. Heat sealing was carried out at 140 °C and a pressure of 400 kPa for 15 seconds by using a Heat-Seal Tester (HST-H3, Labthink Instruments Co., Ltd, Shandong, China), with good sealing performance regardless of the presence of AS powder.

Oxidative stability of almonds was assessed by the peroxide value, conjugated diene and triene content and fatty acid index. These were measured on the almonds at start-up and every 2 months up to a total storage time of 6 months. For these analyses, the oil from the ground almonds were extracted using a Soxhlet with petroleum ether (40–60 °C) for 6 hours.

2.5.1 Peroxide index analysis. The peroxide value of almond oil was determined following the titration procedure described in Commission Regulation.[31] One gram of oil was dissolved in 30 mL of an organic solvent mixture (acetic acid : 1-decanol, 3 : 2 v/v). Then, 200 μL of saturated potassium iodide solution was added, and the mixture was kept in the dark for 1 min. After adding 30 mL of distilled water, the liberated iodine was titrated with 0.01 N $Na_2S_2O_3$. Analyses were performed in triplicate, and the results were expressed as milliequivalents of active oxygen per kilogram of fat (eqn (4)).

$$\mathrm{IP}\left(\mathrm{meq}\frac{O_2}{kg}\right) = \frac{(V - V_0) \times N \times 1000}{M} \tag{4}$$

where V is the volume of 0.01 $Na_2S_2O_3$ used for the sample (mL), V_0 is the volume of the blank (mL), N is the normality of the solution, M is the mass of oil (g), and 1000 is the conversion factor.

2.5.2 Analysis of conjugated dienes and trienes. Conjugated diene and triene contents were determined according to Commission Regulation (EEC).[31] Precisely weighed almond oil samples (0.05 and 0.25 g) were dissolved in 25 and 10 mL of isooctane, respectively, for diene and triene analyses, and their absorbance at 232 and 268 nm, respectively, was recorded in a quartz cuvette using a UV-vis spectrophotometer (Thermo Scientific Evolution 201, Brooklyn, WI, USA). All measurements were performed in triplicate. The results were expressed as specific extinction coefficients (eqn (5)).

$$K_\lambda = \left(\frac{E_\lambda}{c \times s}\right) \tag{5}$$

where K_λ is the specific extinction coefficient, E_λ is the absorbance, c is the solution concentration (g/100 mg), and s is the cuvette trough thickness (cm).

2.5.3 Analysis of oil acidity. The acidity of the almond oil was determined according to Commission Regulation (EEC).[31] A 1 : 1 (v/v) mixture of 96% ethanol and diethyl ether was titrated with 0.1 N KOH, using phenolphthalein as the indicator. After this blank titration, the oil (1 g in 25 mL) was incorporated into the mixture and titrated with 0.1 N KOH until the colour changed. All measurements were carried out in duplicate, the acidity value was calculated applying (eqn (6)), and the results were expressed in mg KOH per g of oil.

$$\text{Acidity value} = \frac{V \times N \times 56,1}{m} \tag{6}$$

where V is the volume of KOH (ml), N is the normality, 56.1 is the molar mass of KOH (g mol^{-1}), and m is the mass of oil (g).

2.6 Statistical analysis

Data were analysed by ANOVA using Statgraphics Centurion XVII-X64 (Statgraphics Technologies, Rockville, MD, USA), and mean differences were compared with Fisher's least significant difference at 95% confidence level.

3 Results and discussion

3.1 Microstructure of films

Blending of PVA with PLA (75 : 25) was done as previously described,[20,32,33] which modified the typical cryofracture of neat PLA and PVA, introducing heterogeneity typical of non-miscible polymers. Fig. 1 shows FESEM images of the film cross-section at different magnification levels, where the PLA phase appeared finely dispersed as almost spherical particles in the PVA continuous phase. Nevertheless, good PLA dispersion and interfacial adhesion were observed, as described in previous studies for PVA/PLA blends with up to 15% PLA.[17] This good dispersion can be attributed to the hydrogen bonding

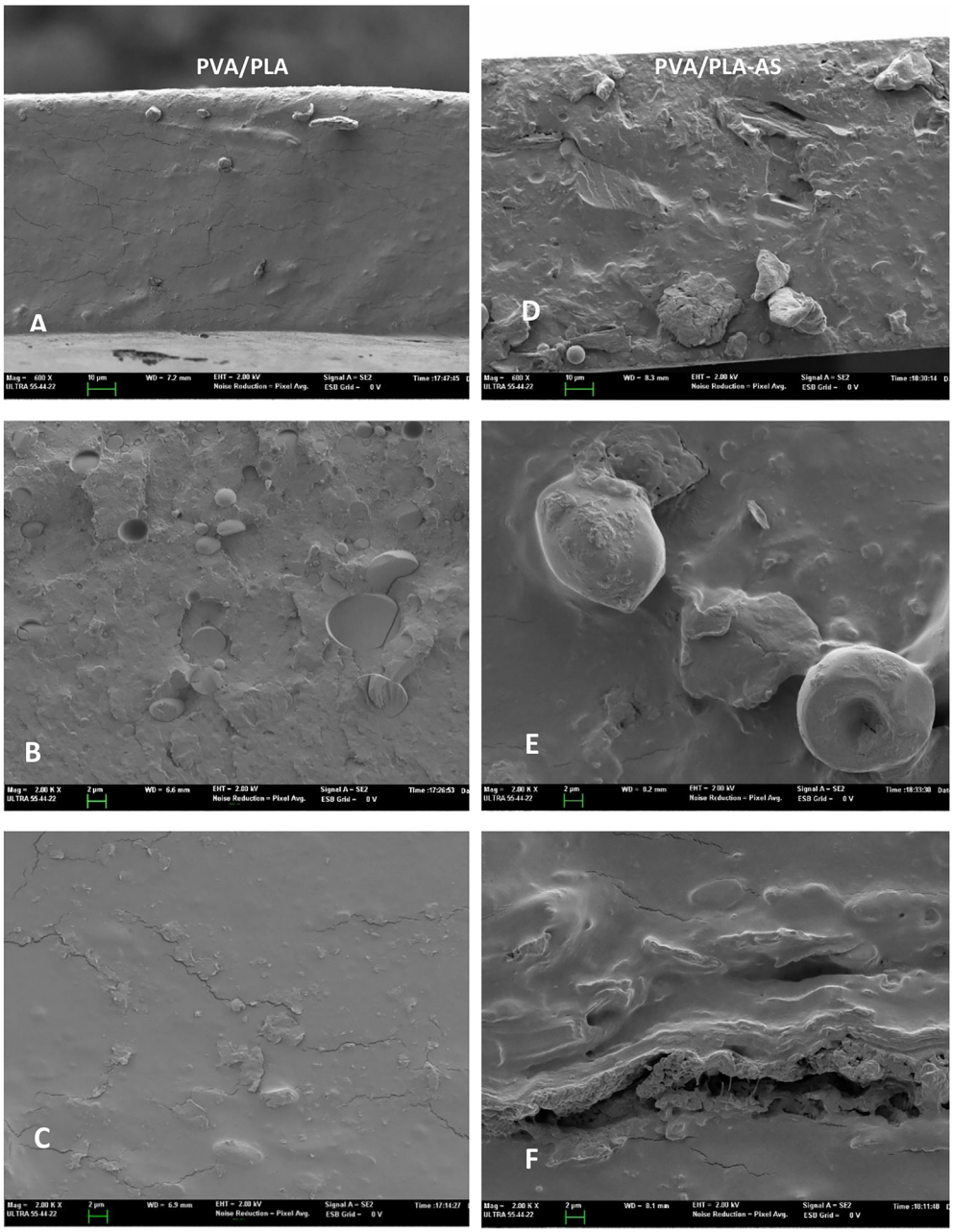

Fig. 1 FESEM micrographs of the cross-section of PVA/PLA films (left) and PVA/PLA-AS (right) films at lower (600×, A and D) and higher (×2000, B, E, C and F) magnifications.

interactions between the PLA carbonyls and PVA hydroxyls, as reported by Liu *et al.*,[17] which affected the PVA interchain hydrogen bonds and thereby the melt viscosity and polymer dispersibility and processability.[18]

Incorporation of AS powder increased the heterogeneity of the films by introducing a new dispersed phase composed of lignocellulosic particles of AS. Fig. 1D–F display the FESEM images of these films at different magnifications, showing the morphology of some dispersed particles which are predominantly fibrous due to the high cellulose content (around 30%) of the almond skin.[24] The AS particles were homogeneously dispersed and appeared better embedded in the polymer matrix than in the mono-polymer films.[24] This suggests better interactions of the AS particles with the blended polymers, probably due to the establishment of a more suitable balance between hydrophobic and hydrophilic interactions in the matrix.

3.2 Phase transitions of polymers

Thermal analysis was performed to characterise the phase transitions of the obtained films. The DSC thermograms obtained from the second heating cycle of different films are shown in Fig. 2, while typical thermal parameters are summarised in Table 2. Semicrystalline PLA did not crystallise

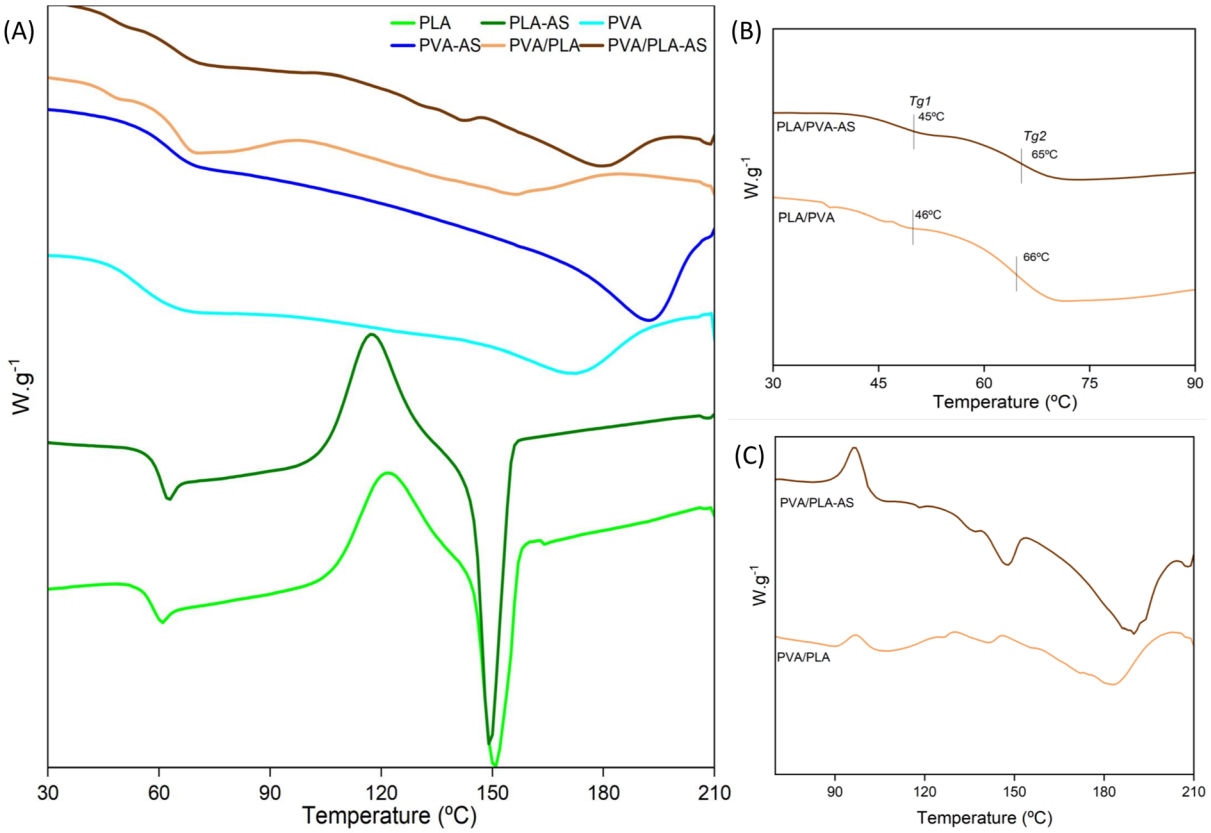

Fig. 2 (A) DSC thermograms (second heating step) for PLA, PVA and PVA/PLA blends with or without AS powder. (B) Expansion of glass transitions for PVA/PLA blend films with and without AS powder. (C) Expansion of the cold crystallisation and melting zones of PLA of blend films in the first heating step.

Table 2 Glass transition temperature, crystallisation temperature, melting temperature, and melting enthalpy of PVA and PLA in mono-polymer and blend films with and without almond skin powder

Polymer	T_c (°C)	T_g (°C)	T_m (°C)	ΔH_m (J g^{-1} polymer)
Mono-polymer films				
PLA	118.0 ± 1.0[a]	59.4 ± 0.3	150.0 ± 0.8	Near zero[b]
PLA-AS	123.0 ± 1.4[a]	57.5 ± 0.2	150.9 ± 0.4	Near zero[b]
PVA	129.3 ± 0.5	55.1 ± 0.2	172.1 ± 0.7	22.9 ± 0.2
PVA-AS	161.4 ± 0.6	59.5 ± 1.5	191.1 ± 0.9	36.0 ± 2.4
PVA/PLA blend films				
PLA	96.3 ± 1.5[a]	46.2 ± 1.5	140.0 ± 0.4	Near zero[b]
PLA (+AS)	97.5 ± 1.3[a]	45.6 ± 0.4	147.0 ± 0.3	Near zero[b]
PVA	96.2 ± 2.4	66.1 ± 0.1	156.9 ± 0.1	12.5 ± 3.2
PVA (+AS)	144.8 ± 2.5	65.5 ± 0.3	177.5 ± 0.9	36.7 ± 8.5

[a] Cold crystallisation temperature. [b] Balance of cold crystallisation and melting enthalpies.

during cooling but exhibit cold crystallisation at T_{cc} about 120 °C, above the glass transition temperature, as previously described.[17] The crystalline forms showed a main melting peak at about 150 °C (T_m in Table 2). The neat enthalpy values considering the balance of crystallisation and melting process revealed that no detectable fraction of the polymer crystallised in the films during cooling. The glass transition of PLA films occurred at 59 °C (T_g, mid-point), which agrees with previous reports by other authors.[34,35] The incorporation of almond skin did not produce noticeable changes in the thermal behaviour of the polymer, and no significant differences were observed in T_g, or crystallisation/melting behaviour.

The PVA films also showed the thermal transitions previously described for this polymer grade equilibrated at 0% RH.[20,24] Incorporation of AS powder produced a slight increase in T_g values relative to the control sample, which can be attributed to the partial adsorption of glycerol by the AS powder, reducing its availability for plasticizing the polymer.[24] The AS filler also affected the PVA crystallisation/melting behaviour, enhancing the crystallisation degree and crystal growth while decreasing the supercooling during crystallisation (higher T_c, T_m and ΔH_m values, as shown in Table 2). Therefore, a nucleating effect can be deduced for the AS particles in the PVA matrix, as reported in previous studies.[24]

In PVA/PLA matrices, an extended double glass transition was observed corresponding to the partially overlapped transition of both polymers (Fig. 2B), with their midpoints shifted with respect to those of the corresponding neat polymers. This could suggest partial miscibility of both polymers, generating two amorphous phases of each polymer containing small amounts of the other polymer. Considering the proportions of both in the blend, the first and smallest change in specific heat

would correspond to the PLA-rich phase and the second to the PVA-rich phase. Thus, PLA was more plasticised in the blend films while PVA was anti-plasticised. This could also be attributed to the partial glycerol migration from PVA (where it was initially incorporated) to the PLA phase during melt blending. Likewise, the PLA cold crystallisation and typical melting peaks of both polymers can be observed in the thermogram (Fig. 2A), where the T_{cc} and T_m of PLA were significantly lower than the values observed in the pure polymer. This reflects the formation of smaller crystals but at a lower temperature, which could be related to the lower T_g values of the PLA rich phase.

Coherent with the partial miscibility of polymers, crystallisation of PVA also occurred at a lower temperature than in the neat polymer (Table 2), revealing more supercooling requirements, while its crystallinity degree was lower due to the blending effect. Chuaponpat *et al.*[36] also observed partial miscibility of PLA and PVA in blend matrices, with the same effect on crystallisation and melting behaviour of PLA and PVA. The incorporation of AS powder into PLA/PVA films had little effect on the thermal transitions of PLA, but this was noticeable in the case of PVA. As observed in the pure polymer, AS produced an increase in the crystallisation temperature, melting temperature and enthalpy of PVA, which also confirms its nucleating effect on the PVA phase of the blends. On a much smaller scale, a similar effect can also be observed in the PLA phase, which was more clearly visible in the first heating thermogram (Fig. 2C), where the successive recrystallisation–melting processes of PLA can be observed, slightly overlapping with the PVA melting. This recrystallisation behaviour of PLA was described by Zhang *et al.*,[37] by using WAXD and DSC analyses and involves crystalline phase transition from α' to α phase.

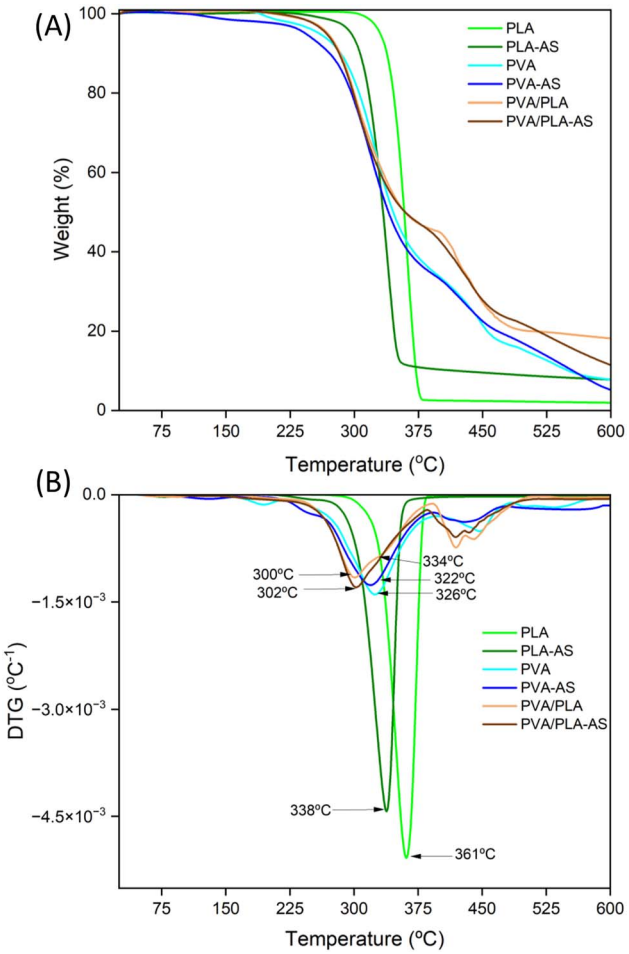

Fig. 3 TGA (A) and DTG (B) curves of PVA, PLA and PVA/PLA films with and without AS powder.

3.3 Thermal stability of films

Thermogravimetric analysis (TGA) was performed to investigate the impact of AS incorporation on thermal stability of both polymers (Fig. 3). Semi-crystalline PLA showed a primary degradation peak at 361 °C (maximum degradation rate), in line with that reported by other authors.[38] The addition of almond skin caused a decrease in this temperature (T_{peak}: 338 °C), suggesting partial hydrolysis of the polymer chains during film processing due to bound water released from the AS filler.[24] In both PVA and PVA/PLA films, a small weight loss was observed from 125 to 250 °C that was attributed to the volatilisation or degradation of glycerol.[39] The maximum degradation temperature of PVA (main peak in the DTG curve) was observed 326 °C, while the addition of AS did not significantly alter this value, as observed in previous studies on PVA reinforced with different hydrophilic fillers, such as cellulose fibres.[20,40]

The PVA/PLA blends showed degradation curves close to the PVA pattern, according to the higher ratio of this polymer, but exhibiting a double degradation peak (DTG) between 275 °C and 375 °C. It showed a primary maximum at 300 °C below that of neat PVA and a secondary maximum at 334 °C close to but lower than that of neat PLA. This behaviour also points to the partial miscibility of both polymers, since no clearly separated degradation steps were observed, but practically overlapped with two maxima degradation rates corresponding to the PVA-rich and PLA-rich phases at 302 °C and 334 °C, respectively (Fig. 3B). Incorporation of AS (15%) into the PVA/PLA film hardly affected the degradation curve of the blend.

3.4 FTIR spectroscopy analysis

The FTIR spectra of the neat polymers and their blend, with and without AS powder, are shown in Fig. 4. Neat PLA films exhibited typical vibration bands associated with the carbonyl (C═O) stretching vibration at 1740 cm^{-1}, the C–O stretching between 1180 and 1080 cm^{-1} and the asymmetric and symmetric CH_3 stretching vibrations at 2995 and 2945 cm^{-1}.[24,41] For neat PVA films, the characteristic vibration bands previously described[20] were also observed, with a broad and intense absorption band at 3200–3400 cm^{-1} corresponding to O–H stretching, the peaks at 2910 and 2858 cm^{-1} attributed to the stretching vibrations of the C–H and –CH_2 groups and a characteristic broad peak between 1700 and 1730 cm^{-1}attributed to the C═O vibration of the residual acetate groups of PVA. This broad peak was associated with the hydrogen-bonded and non-

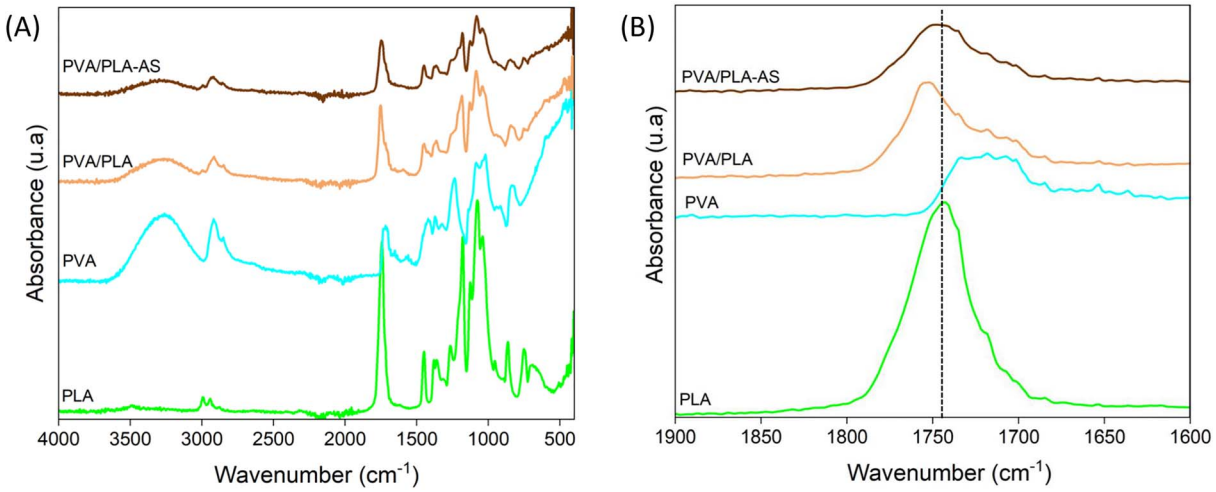

Fig. 4 (A) FTIR spectra of PLA, PVA and PVA/PLA blends with or without AS powder. (B) Expansion of the carbonyl region (1500–2000 cm^{-1}).

hydrogen-bonded carbonyls within the matrix according to the different degrees of chain association by hydrogen bonds.[42]

In the PVA/PLA (75 : 25) blend films, overlapping of the vibration of both polymers was observed, as expected, but the spectra showed a higher degree of similarity to pure PVA that constitutes the continuous and major phase of the blend films. However, as shown in the expanded carbonyl region (Fig. 4B), the C═O stretching vibration band of PLA was clearly observed in the blend films but slightly shifted to 1748 cm^{-1} while exhibiting a prominent shoulder associated with C═O stretching of residual acetate groups of PVA chains that are present in a lower ratio in the blend (PVA hydrolysis degree: 87–90%). These changes confirmed the interactions between PLA and PVA chains in the blend films deduced from thermal analysis, which could be mainly established though hydrogen bonds between the PLA carbonyls and PVA hydroxyls.

The incorporation of AS powder into the blend films did not result in any notable changes in the films' spectra, as no new bands were observed, probably due to the relatively low concentration of AS compounds in the film. However, the shift of the PLA C═O band in these films was slightly lower (1742 cm^{-1}) than that of the PVA/PLA films. This suggests that PVA–PLA interactions were more limited when AS particles were present in the mixture, probably due to the competitive interactions between PVA and AS particles described in a previous study.[24]

3.5 Barrier properties of films

Table 3 shows the oxygen permeability (OP) and water vapour permeability (WVT) of neat PLA and PVA films and their blends with or without AS powder. PLA showed a significantly higher oxygen permeability than PVA, as previously reported,[25,32] which is attributed to the high oxygen solubility in the hydrophobic PLA matrix. In contrast, PVA has a uniform crystalline structure and low oxygen solubility within its polar matrix, which reduces the oxygen transport through the matrix.[43] Oppositely, PVA films exhibited higher WVP than PLA films due to its hydrophilic nature and high moisture sensitivity, which promote water uptake and enhance vapour transport. Incorporation of AS lowered the OP values of both polymers by approximately 25% in PLA and 17% in PVA by promoting the tortuosity factor in the matrix for mass transport, while the present AS antioxidants could act as oxygen scavengers.[24] In contrast, AS particles were less effective at increasing the water vapour barrier capacity of the films. In PVA films, AS powder produced only 8% reduction in WVP, whereas in PLA films WVP was duplicated. The promotion of PVA crystallinity when AS particles were present in the matrix will contribute to the enhancement of barrier capacity against water vapour and oxygen of PVA films. Espinosa *et al.*[44] also observed a reduction in the WVP and OP of PVA composites with lignocellulosic fillers, depending on their ratio in the film, the aspect ratio of fibres, and the lignin content.

The PVA/PLA blend films exhibited OP and WVP values comparable to PVA films due to PVA continuous phase in the film, which mainly controls mass transport. Dispersed PLA domains in the PVA matrix create hydrophobic pathways that

Table 3 Average values of oxygen permeability (OP) and water vapour permeability (WVP) of the mono-polymer PLA and PVA films and their PVA/PLA blend (75 : 25), with and without AS powder

Sample	OP × 10^{14} (cm^3 m^{-1} s^{-1} Pa)	WVP × 10^{11} (g Pa^{-1} s^{-1} m)	Thickness (mm)
PLA	189.4 ± 1.5^{a1}	2.7 ± 0.8^{d2}	0.190 ± 0.005^{a1}
PLA-AS	143.0 ± 8.0^{b2}	5.9 ± 0.9^{d1}	0.170 ± 0.020^{b1}
PVA	11.5 ± 0.8^{cd1}	219.0 ± 5.0^{a1}	0.180 ± 0.010^{b1}
PVA-AS	9.5 ± 0.1^{cd2}	202.0 ± 8.0^{b2}	0.180 ± 0.008^{b1}
PVA/PLA	18.0 ± 3.0^{c1}	113.0 ± 9.0^{c1}	0.130 ± 0.013^{d2}
PVA/PLA-AS	6.5 ± 0.8^{d2}	122.0 ± 10.0^{c1}	0.150 ± 0.018^{c1}

[a,b,c] Different letters in the superscript indicate significant differences between samples ($p < 0.05$). [1,2] Different numbers in the superscript indicate significant differences between a determined formulation with and without AS ($p < 0.05$).

slightly enhanced the oxygen permeation while decreasing the permeation of water molecules. The WVP of the PVA/PLA film was reduced by 48% with respect to neat PVA films, whereas the OP increased by 53%. The incorporation of AS powder into the PVA/PLA blend reduced the OP by 64% relative to the control blend, while it not significantly affected the WVP of the control blend. Therefore, AS particles were more effective at reducing the OP in blend films than in neat PLA or PVA films, while the WVP values remained lower than that of pure PVA (44% reduction). The increase of PVA crystallinity by the nucleating effect of AS particles deduced from DSC analysis will contribute to the best barrier performance of composite films compared to the control blend film. Therefore, the PVA/PLA-AS films exhibited the best oxygen barrier properties, while their water vapour barrier capacity was highly improved compared to that of neat PVA films.

Many factors determine the effect of lignocellulosic fillers on the barrier properties of the composites, such as the crystallinity degree of fibres, the content of less polar compounds and their potential diffusion and interaction within the polymer matrix, and the morphology and surface properties of fibres.[45,46] Likewise, this effect depends largely on the filler ratio and the nature of the continuous polymer matrix. At a relatively low ratio (below 5%) lignocellulosic fillers reduced the WVP and OP in hydrophobic polyesters, such as PLA or PHB.[47] At high ratios, these fillers may have different effects on hydrophilic matrices (chemically more compatible with the fillers) and hydrophobic polymers. In the former, fillers generally reduced the WVP and OP mainly due to the improved tortuosity factor for mass transfer, mainly induced by the high crystallinity of the particles.[48] Conversely, in hydrophobic polymeric matrices, such as PLA, these promoted water transfer, as they act as accelerators of the passage of water molecules, having an opposite effect on the OP value.[49,50] The AS particles reduced the WVP of neat PVA by 8%, whilst they had no significant effect on the WVP of the PVA/PLA blend, where they would have an opposite effect on each of the polymer phases.

3.6 Optical properties of films

The internal transmittance (T_i) of the film samples in the UV-visible range (200–800 nm) is shown in Fig. 5. The highest transmittance values were observed for the neat PLA and PVA films, in line with their structural homogeneity and intrinsic optical transparency. The incorporation of the AS powders greatly reduced the film transmittance, mainly in the UV region. This reduction reflects the light scattering effect induced by dispersed particles and the selective light absorption by chromophores of AS constituents (mainly phenolic compounds). The greater optical effect of AS particles on the PLA matrix could be related to their poorer integration, giving rise to a more heterogeneous structure, as shown in FESEM images. The decreased transparency provided the films with a beneficial barrier against light-triggered oxidation.[20,51]

The PLA/PVA blend exhibited lower transparency due to its more heterogeneous structure with PLA-rich particles dispersed within the continuous PVA matrix, as shown in the FESEM images. Differences in the refractive index of the polymer phases caused light scattering, reducing the transparency. Incorporation of AS powder further decreased the film transparency, as observed in neat PLA and PVA films and also reported by other authors for lignocellulose biocomposites.[51,52]

Light interactions with different polymer matrices produced different colours in the films, whose chromatic locust can be observed in Fig. 5B, where the respective lightness values were also marked, along with the film images. Neat PLA and PVA films showed the highest lightness values, but they were highly

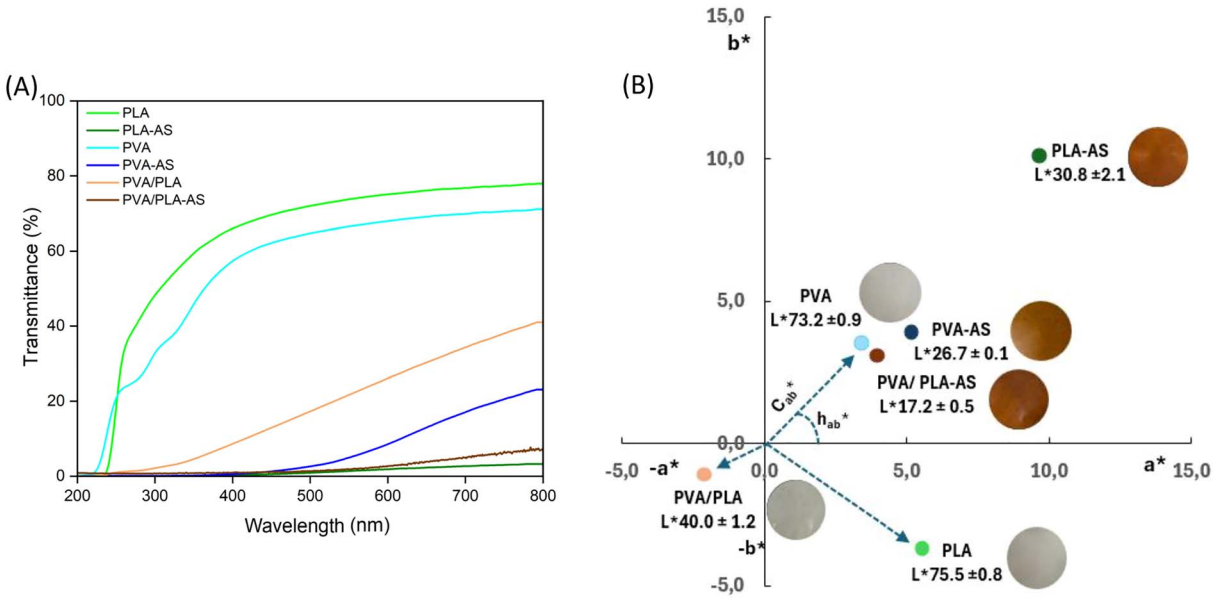

Fig. 5 Internal transmittance spectra in the visible range of different PLA and PVA films and their PVA/PLA blend (75 : 25), without and with 15% almond skin. (B) Chromatic plane a^*b^*showing the locations of different PLA and PVA films and their PVA/PLA blend (75 : 25), without and with 15% almond skin, and their luminosity values (L^*).

darkened by AS incorporation, while the colour was more saturated (mainly in PLA films), and the hue shifted towards orange reddish tones. The PVA/PLA blend films were slightly darker than the mono-polymer films due to the lower light transmission capacity previously discussed. The addition of AS particles to blend films further reduced the L^* values, with similar effects on the chromatic parameters. This increase in colour saturation with AS particles must be attributed not only to the natural pigments of the almond skin but also to the formation of coloured compounds during heat treatment, driven by Maillard and caramelisation reactions at high temperatures.[25]

3.7 Mechanical properties of films

Table 4 summarises the mechanical properties obtained from the stress–strain curves of the films. PLA films with AS showed an elastic modulus (EM) similar to neat PLA, but the fracture resistance (TS) decreased by 35%, and the extensibility (E) decreased by 32%. Incorporation of AS powder into PVA films also decreased the values of TS and E by 52% and 32%, respectively, without significant effect on the EM values. This was also observed for other lignocellulosic fillers due to the disruption of the matrix continuity and limited compatibility with the polymer.[24,53] The reinforcing properties of lignocellulosic fillers in PLA were only observed at low filler contents (below 3%),[47] whereas in PVA composites this effect was observed across a wider range of concentrations.[44]

The PVA/PLA films showed a tensile behaviour closer to that of PVA films, with the continuous PVA phase dominating the composite properties. Dispersed PLA reduced the elastic modulus, resistance to fracture and extensibility by 44%, 73% and 71%, respectively, reflecting the weakening effect of the PLA domains and polymer interactions on the cohesion forces of the PVA continuous matrix, which, in turn, have a lower crystallinity degree than neat PVA films. However, the addition of AS powder to the PVA/PLA blend film increased the elastic modulus by 233%, while it maintained the resistance to fracture of the blend matrix and reduced its extensibility by 50%. These effects can be attributed in part to the increase in the crystallinity of PVA caused by the AS particles. Therefore, a more remarkable reinforcing effect of AS particles was observed in blend PLA/PVA films than in mono-polymer films. This can be attributed to the lower crystallinity of PVA in the blend films and to its significant increase by the effect of the AS filler. Overall, almond skin powder improved the mechanical performance of the PVA/PLA composite, limiting only its plastic deformation capacity, yet remaining superior to pure PLA films. The reinforcing effect of lignocellulosic fibres depends on its stiffness and crystallinity, the interfacial adhesion of the fibre and the polymer, and the involved force transmission mechanisms within the composite, affected by the structural arrangement.[53] The obtained results suggest that almond skin particles could contribute to polymer compatibilization, enhancing interfacial adhesion and mechanical performance of the biocomposite. This may also be due, in part, to the increased crystallinity of PVA.

Table 4 Tensile parameters (elastic modulus: EM, tensile strength: TS and strain at break: E%) of different PLA, PVA and PVA/PLA films with 0 and 15 wt% almond skin powder

Sample	EM (MPa)	TS (MPa)	E (%)
PLA	1360 ± 60^{a1}	50.0 ± 2.0^{a1}	5.0 ± 0.4^{d1}
PLA-AS	1306 ± 70^{a1}	32.4 ± 0.9^{bc2}	3.4 ± 0.4^{d2}
PVA	123 ± 7^{bc1}	44.0 ± 7.0^{ab1}	85.1 ± 0.6^{a1}
PVA-AS	110 ± 15^{bc1}	21.0 ± 4.0^{cd2}	58.0 ± 11.0^{b2}
PVA/PLA	69 ± 3^{c2}	12.0 ± 0.7^{d1}	25.0 ± 0.3^{c1}
PVA/PLA-AS	230 ± 30^{b1}	11.7 ± 1.6^{d1}	12.0 ± 4.0^{cd2}

^{a,b,c} Different letters in superscript indicate significant differences between samples ($p < 0.05$). ^{1,2} Different numbers in superscript indicate significant differences between samples with and without AP ($p < 0.05$).

In summary, PLA/PVA (75 : 25) composite films containing AS powder exhibited the highest oxygen barrier performance at 53% RH (OP: 6.5×10^{-14} cm^3 m^{-1} s^{-1} Pa), successfully outperforming some high barrier synthetic reference materials, such as PET (OP = 11.4–57.1 $\times 10^{-14}$ cm^3 m^{-1} s^{-1} Pa)[54] and approaching the ultra-high oxygen barrier range of commercial EVOH (OP = 2.3–11.4 $\times 10^{-14}$ cm^3 m^{-1} s^{-1} Pa) depending on the material characteristics.[55] These films also had better water vapour barrier capacity and mechanical properties than pure PVA films, which constitutes a notable advantage for the packaging of dry, oxidation-sensitive products, such as roasted almonds.

Likewise, although the films were obtained at the laboratory-scale, their thermoprocessing is relatively close to the continuous process techniques applied at the industrial level. Specifically, the blending process could be carried out by extrusion, fitting the process conditions in the temperature and shear conditions range of the study, to obtain pellets of the corresponding master batch. These pellets could be subject to extrusion casting to obtain films and bags using adequate heat-sealing conditions.

In the next section, analysis of the antioxidant potential of these films that can be associated with the high phenolic content of the filler is presented.

3.8 Antioxidant capacity of the films in packaged toasted almonds

The development of oxidative deterioration and the quality loss of toast almonds packaged in PVA/PLA bags with and without AS powder were assessed by determining the peroxide value, the levels of conjugated dienes and trienes, and the acidity index of the extracted oil, throughout the storage time at 25 °C (Fig. 6). The peroxide index (PI) indicates the hydroperoxide compounds formed as initial oxidation products of the unsaturated fatty acids present in the sample.[56,57] The initial value of the oil extracted from the almonds was 2.53 ± 0.80 meq O_2 per kg oil, similar to values observed in previous studies,[58,59] indicating the high quality of the product with respect to its lipid oxidation status. During storage (Fig. 6A), the peroxide value of almond oil increased progressively, reflecting the natural oxidation process influenced by multiple factors, including storage temperature

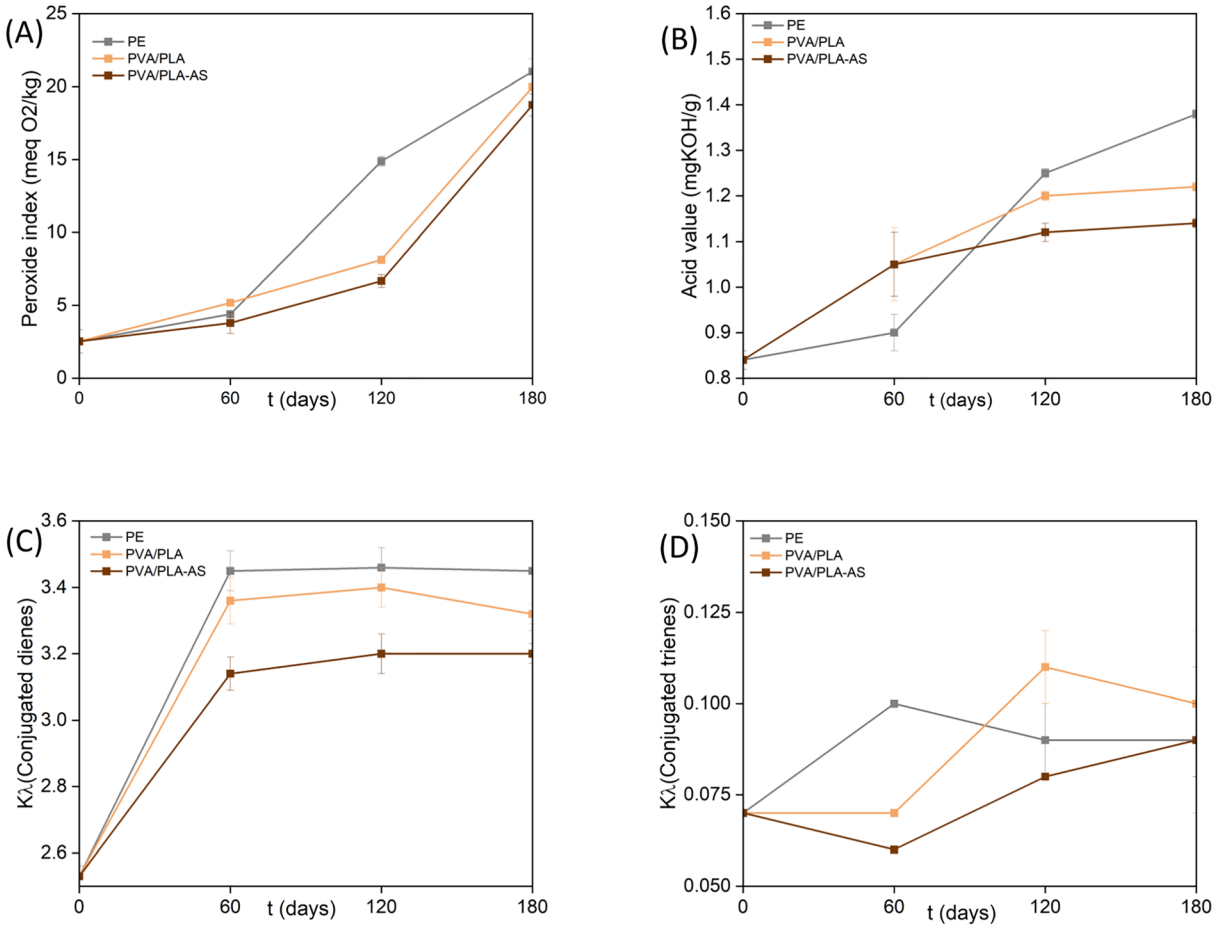

Fig. 6 Development of peroxide value (A), total acid value (B), and extinction coefficient values of conjugated dienes (k232) (C) and trienes (k268) (D) throughout the storage of almond oil extracted from toast almonds packed in bags of PVA/PLA films with 0 and 15 wt% almond skin powder, compared with the PE control.

and time, the unsaturated fatty acid composition of the oil, and packaging conditions that affect the internal oxygen pressure, and light transmission which can catalyse oxidation.[59] Fig. 6A shows that samples packaged in PVA/PLA-AS bags had lower peroxide values than those packaged in PVA/PLA or PE controls throughout the whole storage period. In PE samples, the lower OP values at 180 storage days than that expected from the previous control suggests the start of their decomposition with the progress of the oxidative process and the formation of secondary oxidation products.[59] The greatest protective effect of PVA/PLA materials would be related to their greater oxygen barrier capacity, and, in the case of PVA/PLA-AS bags, to the additional UV-light blocking effect and the antioxidant activity of almond skin compounds, especially phenols.[23,60] The phenolic compounds present in almond skin are able to act as radical neutralisers and hydrogen donors, effectively stopping oxidative chain reactions in the early stages of lipid deterioration.[61] In fact, almond skin effectively protects almonds from oxidation since peeled almonds oxidize faster than the non-peeled fruit.[62] Nevertheless, diffusion of antioxidants from the almond peel in the bag to the packaged almonds was not expected, and the observed protection must be attributed to the oxygen scavenging effect in the packaging promoted by the AS antioxidants. Fresh oils typically have a PV below 10 meq kg^{-1} (ref. 58), and both PVA/PLA and PVA/PLA-AS films maintained the PV index of packaged almonds below this value for up to 120 days.

Oil acidity is a critical parameter that determines the physicochemical quality of the oil, quantifying the free fatty acids generated through triglyceride hydrolysis.[63] As shown in Fig. 6B, the initial value was 0.98 ± 0.19 mg KOH per g of oil, confirming an initial state with no relevant evidence of acylglyceride hydrolysis.[58] Throughout the storage, the acidity index increased in different samples, and from 4 months onwards, lower values were observed for the samples packaged in PVA/PLA-AS films. After six months, the acidity of oil in samples packaged in PVA/PLA-AS films was 17 and 13% lower than those packaged in PE and PVA/PLA materials, respectively. Activity of lipases responsible for triglyceride hydrolysis did not require oxygen, but oxygen affects the stability of substrates, while a limited oxygen pressure can reduce the synthesis of lipases or their activity.[64]

Fig. 6C and D show the progress of conjugated diene and triene species resulting from the oxidative degradation of fatty acids. Conjugated dienes are formed by the migration of double bonds within polyunsaturated fatty acids during the initial

stages of peroxide development, resulting in a distinctive absorption peak at 232 nm.[65] Conjugated trienes, produced during secondary oxidation pathways, exhibit a maximum absorption peak at 268 nm.[66] Consequently, spectrophotometric evaluation at 232 and 268 nm serves as an effective tool for assessing the degree of oil oxidation. The oil initially showed a diene value of 2.525 ± 0.027, characteristic of a low oxidative state. Over time, the levels increased to 3.45 3.32, and 3.20 in PE, PVA/PLA, and PVA/PLA-15 bags, respectively. The evolution of these values is consistent with the peroxide values, as both parameters are indicators of primary oxidation.[24] The triene concentration showed only slight variations during the six-month storage period, increasing from 0.07 to 0.09, with no significant differences among packaging types. This suggests that oxidation did not progress sufficiently into secondary stages and that both, storage conditions and oil composition, limited the formation of these compounds. Furthermore, the presence of antioxidants in materials (PVA/PLA-AS) contributed to prolonging the oxidative stability of toast almonds, further reducing the progression of primary oxidation.[67]

4 Conclusions

PVA/PLA blend films were obtained by melt blending; thermal analyses revealed partial miscibility between the polymers, which favored interfacial adhesion and ensured a good dispersion of PLA within the PVA continuous phase. Two amorphous phases were observed in the blend film, corresponding to a PLA rich phase with a lower T_g than the neat polymer, and a PVA-rich phase with a higher T_g than that of neat PVA. This could also be attributed to the final partition of glycerol initially incorporated in the PVA phase during melt blending. Crystallisation of the polymers was also affected by the blending effect that reduced the crystallisation temperature of PVA and the cold crystallisation temperature of PLA. Coherently, the melting temperature and enthalpy of PVA were lower in blend films suggesting that interactions with PLA inhibited PVA crystallisation and crystal growth. In every case, PLA was not crystallised in the films since a near zero balance was obtained for the cold crystallisation and melting enthalpies. Incorporation of AS powder into the blend films did not significantly affect the glass transition of both polymer phases, but enhanced crystallisation and crystal growth of PVA, increasing its T_c, T_m and ΔH_m, with respect to the AS-free film, as also occurred in neat PVA films.

PLA reduced the WVP of PVA by about 50%, while increasing the OP (56%) in the blend films. Nevertheless, the incorporation of AS powder brought the OP values of blend films to lower values than those of neat PVA films, without a significant increase in WVP. Likewise, AS powder promoted the stiffness of the blend films (by 233%) reducing their extensibility (by 50%), but without significant effect on the resistance to break. Moreover, the PLA/PVA-AS films reduced the oxidation rate of packaged toast almonds during storage at 25 °C and 53% RH for 6 months, in comparison with the AS-free film and PE controls. Therefore, PVA/PLA-AS films represent a sustainable alternative for packaging low moisture foods sensitive to oxidation while contributing to valorisation of a highly produced agri-food waste, in the frame of circular economy.

Author contributions

Irene Gil-Guillén: writing – original draft, visualization, methodology, investigation. Chelo González-Martínez: methodology, supervision, conceptualisation, funding acquisition. Amparo Chiralt: writing – review & editing, visualization, supervision, methodology, funding acquisition, conceptualization.

Conflicts of interest

The authors declare that they have no known competing financial interests or personal relationships that could have appeared to influence the work reported in this paper.

Data availability

The data necessary to reproduce the results of this research are available on reasonable request.

Acknowledgements

This research was funded by the Next Generation Funds of the Comunitat Valenciana (GVANEXT) PRTR-C17.I1, Ministry of Science, Innovation and Universities: AGROALNEXT/2022/026, and Generalitat Valenciana: CIPROM/2021/071.

References

1 E. Hwang, Y.-H. Yang, J. Choi, S.-H. Park, K. Park and J. Lee, Biodegradable plastics as sustainable alternatives: advances, basics, challenges, and directions for the future, *Materials*, 2025, **18**, 4247.
2 S. Nanda, B. R. Patra, R. Patel, J. Bakos and A. K. Dalai, Innovations in applications and prospects of bioplastics and biopolymers: a review, *Environ. Chem. Lett.*, 2022, **20**, 379–395.
3 O. Olatunji, *Re-envisioning Plastics Role in the Global Society: Perspectives on Food, Urbanization, and Environment*, Springer, 2024.
4 E. Athanasopoulou, D. M. Power, E. Flemetakis and T. Tsironi, Towards the rational use of plastic packaging to reduce microplastic pollution: a mini review, *J. Mar. Sci. Eng.*, 2025, **13**, 1245.
5 K. Syberg, M. B. Nielsen, N. B. Oturai, L. P. W. Clausen, T. M. Ramos and S. F. Hansen, Circular economy and reduction of micro(nano)plastics contamination, *J. Hazard. Mater. Adv.*, 2022, **5**, 100044.
6 K. Amulya, B. Katakojwala, S. Ramakrishna and S. V. Mohan, Low carbon biodegradable polymer matrices for sustainable future, *Compos., Part C: Open Access*, 2021, **4**, 100111.
7 D. Gere and T. Czigany, Future trends of plastic bottle recycling: compatibilization of PET and PLA, *Polym. Test.*, 2020, **81**, 106160.

8 M. Qin, C. Chen, B. Song, M. Shen, W. Cao, H. Yang, *et al.*, A review of biodegradable plastics to biodegradable microplastics: another ecological threat to soil environments?, *J. Clean. Prod.*, 2021, **312**, 127816.
9 R. Ṣomoghi, S. Mihai and F. Oancea, An overview of bio-based polymers with potential for food packaging applications, *Polymers*, 2025, **17**, 2335.
10 M. Shen, B. Song, G. Zeng, Y. Zhang, W. Huang, X. Wen, *et al.*, Are biodegradable plastics a promising solution to solve the global plastic pollution?, *Environ. Pollut.*, 2020, **263**, 114469.
11 O. Plohl, L. Fras Zemljič, A. Erjavec, N. Šep, M. Čolnik, Y. Fan, *et al.*, Decomposition and fragmentation of conventional and biobased plastic wastes in simulated and real aquatic systems, *Clean Technol. Environ. Policy*, 2024, 8569–8584.
12 European Bioplastics, *Bioplastics market data 2025: Global market trends and insights*, European Bioplastics, Berlín, 2025.
13 J. O'Loughlin, D. Doherty, B. Herward, C. McGleenan, M. Mahmud, P. Bhagabati, *et al.*, The potential of bio-based polylactic acid (PLA) as an alternative in reusable food containers: a review, *Sustainability*, 2023, **15**, 15312.
14 N. A. A. B. Taib, M. R. Rahman, D. Huda, K. K. Kuok, S. Hamdan, M. K. Bin Bakri, *et al.*, A review on polylactic acid (PLA) as a biodegradable polymer, *Polym. Bull.*, 2023, **80**, 1179–1213.
15 B. Liu, J. Zhang and H. Guo, Research progress of polyvinyl alcohol water-resistant film materials, *Membranes*, 2022, **12**, 347.
16 R. D. Souza, E. R. Lopes, E. M. Ramos, T. V. Oliveira and C. P. Oliveira, Active packaging: development and characterization of polyvinyl alcohol (PVA) and nitrite film for pork preservation, *Food Chem.*, 2024, **437**, 137811.
17 Z. Liu, H. Lu, H. Zhang and L. Li, Poly(vinyl alcohol)/polylactic acid blend film with enhanced processability, compatibility and mechanical property fabricated via melt processing, *J. Appl. Polym. Sci.*, 2021, **138**, 51204.
18 W. Wang, Y. Gong, Q. Sun, L. Li, A. Xu, R. Liu, *et al.*, High performance polyvinyl alcohol/polylactic acid materials: facile preparation and improved properties, *J. Appl. Polym. Sci.*, 2022, **139**, e52470.
19 S. Fan, H. Mu, H. Gao, H. Chen, W. Wu, X. Fang, *et al.*, Preparation of PVA/PLA-based intelligent packaging to indicate the quality of shiitake mushrooms, *J. Agric. Food Res.*, 2023, **12**, 100589.
20 I. Gil-Guillén, C. González-Martínez and A. Chiralt, Influence of the cellulose purification method on the properties of PVA composites with almond shell fibres, *Molecules*, 2025, **30**, 372.
21 R. Singh, R. Kumar, Pawanpreet, M. Singh and J. Singh, On mechanical, thermal and morphological investigations of almond skin powder-reinforced PLA feedstock filament, *J. Thermoplast. Compos. Mater.*, 2022, **35**, 230–248.
22 M. Barral-Martínez, M. Fraga-Corral, P. García-Pérez, J. Simal-Gandara and M. A. Prieto, Almond by-products: valorization for sustainability and competitiveness of the industry, *Foods*, 2021, **10**, 1793.
23 P. A. V. Freitas, L. Martín-Pérez, I. Gil-Guillén, C. González-Martínez and A. Chiralt, Subcritical water extraction for valorisation of almond skin from almond industrial processing, *Foods*, 2023, **12**, 3759.
24 I. Gil-Guillén, I. Gonçalves, P. Ferreira, C. González-Martínez and A. Chiralt, Biodegradable antioxidant composites with almond skin powder, *Polymers*, 2025, **17**, 2201.
25 L. Martin-Perez, C. Contreras, A. Chiralt and C. Gonzalez-Martinez, Active polylactic acid (PLA) films incorporating almond peel extracts for food preservation, *Molecules*, 2025, **30**, 1988.
26 ASTM International, ASTM E96/E96M Standard test methods for water vapor transmission of materials, 2005.
27 T. H. McHugh, R. Avena-Bustillos and J. M. Krochta, Hydrophilic edible films: modified procedure for water vapor permeability and explanation of thickness effects, *J. Food Sci.*, 1993, **58**, 899–903.
28 ASTM International, ASTM D3985 Standard test method for oxygen gas transmission rate through plastic film and sheeting using a coulometric sensor, 2010.
29 ASTM International, ASTM D882 Standard test method for tensile properties of thin plastic sheeting, 2012.
30 L. M. Franklin, D. M. Chapman, E. S. King, M. Mau, G. Huang and A. E. Mitchell, Chemical and sensory characterization of oxidative changes in roasted almonds undergoing accelerated shelf life, *J. Agric. Food Chem.*, 2017, **65**, 2549–2563.
31 Commission Regulation (EEC) No 2568/91, Off. *J. Eur. Communities*, 1991, **L248**, 1–48.
32 P. A. V. Freitas, N. J. Bas Gil, C. González-Martínez and A. Chiralt, Antioxidant poly(lactic acid) films with rice straw extract for food packaging applications, *Food Packag. Food Packag. Shelf Life*, 2022, **34**, 101003.
33 J. Andrade, C. González-Martínez and A. Chiralt, Physical and active properties of poly(vinyl alcohol) films with phenolic acids as affected by the processing method, Food Packag, *Food Packag. Shelf Life*, 2022, **33**, 100855.
34 M. A. Ortenzi, S. Gazzotti, B. Marcos, S. Antenucci, S. Camazzola, L. Piergiovanni, *et al.*, Synthesis of polylactic acid initiated through biobased antioxidants: towards intrinsically active food packaging, *Polymers*, 2020, **12**, 1183.
35 N. M. Nurazzi, N. Abdullah, M. N. F. Norrrahim, S. H. Kamarudin, S. Ahmad and S. S. Shazleen *et al.*, Thermogravimetric analysis and differential scanning calorimetry of PLA/cellulose composites, in *Polylactic Acid-Based Nanocellulose and Cellulose Composites*, CRC Press, 2022, pp. 145–164.
36 N. Chuaponpat, T. Ueda, A. Ishigami, T. Kurose and H. Ito, Morphology, thermal and mechanical properties of co-continuous porous structure of PLA/PVA blends by phase separation, *Polymers*, 2020, **12**, 1083.
37 J. Zhang, K. Tashiro, H. Tsuji and A. J. Domb, Disorder-to-order phase transition and multiple melting behavior of poly(l-lactide), *Macromolecules*, 2008, **41**, 1352–1357.

38 T. Yang, R. Lu, J. Yan, S. Jin and Y. Xue, Influence of molecular weight on the thermal degradation of polylactic acid: a crystallization perspective, *Polymer*, 2025, **335**, 128839.
39 J. Andrade, C. González-Martínez and A. Chiralt, Antimicrobial PLA-PVA multilayer films containing phenolic compounds, *Food Chem.*, 2022, **375**, 131861.
40 A. A. Rowe, D. J. Tajvidi and D. J. Gardner, Thermal stability of cellulose nanomaterials and their composites with polyvinyl alcohol (PVA), *J. Therm. Anal. Calorim.*, 2016, **126**, 1371–1386.
41 Q. Wang, C. Ji, J. Sun, Q. Zhu and J. Liu, Structure and properties of polylactic acid biocomposite films reinforced with cellulose nanofibrils, *Molecules*, 2020, **25**, 3306.
42 H. Y. Yu, Z. Y. Qin, C. F. Yan and J. M. Yao, Green nanocomposites based on functionalized cellulose nanocrystals: a study on the relationship between interfacial interaction and property enhancement, *ACS Sustain. Chem. Eng.*, 2014, **2**, 875–886.
43 S. Marano, E. Laudadio, C. Minnelli and P. Stipa, Tailoring the barrier properties of PLA: a state-of-the-art review for food packaging applications, *Polymers*, 2022, **14**, 1626.
44 E. Espinosa, I. Bascón-Villegas, A. Rosal, F. Pérez-Rodríguez, G. Chinga-Carrasco and A. Rodríguez, PVA/(ligno) nanocellulose biocomposite films: effect of residual lignin content on structural, mechanical, barrier and antioxidant properties, *Int. J. Biol. Macromol.*, 2019, **141**, 197–206.
45 P. Camarena-Bononad, P. A. V. Freitas, C. González-Martínez, A. Chiralt and M. Vargas, Influence of the purification degree of cellulose from Posidonia oceanica on the properties of cellulose-PLA composites, *Polysaccharides*, 2024, **5**, 807–822.
46 P. H. F. Pereira, M. F. de Freitas Rosa, M. O. H. Cioffi, K. C. C. de Carvalho Benini, A. C. Milanese, H. J. C. Voorwald, *et al.*, Vegetal fibers in polymeric composites: a review, *Polímeros*, 2015, **25**, 9–22.
47 U. Qasim, R. Fatima and M. Usman, Efficient barrier properties of mechanically enhanced agro-extracted cellulosic biocomposites, *Mater. Today Chem.*, 2020, **18**, 100378.
48 I. Benito-González, A. López-Rubio and M. Martínez-Sanz, Potential of lignocellulosic fractions from Posidonia oceanica to improve barrier and mechanical properties of bio-based packaging materials, *Int. J. Biol. Macromol.*, 2018, **118**, 542–551.
49 R. Kumar, S. Kumari, B. Rai, R. Das and G. Kumar, Effect of nano-cellulosic fiber on mechanical and barrier properties of PLA green nanocomposite film, *Mater. Res. Express*, 2019, **6**, 125108.
50 A. Abdulkhani, J. Hosseinzadeh, S. Dadashi and M. Mousavi, Morphological, thermal, mechanical and barrier properties of PLA-based biocomposites prepared with micro and nano sized cellulosic fibers, *Cellul. Chem. Technol.*, 2015, **49**, 597–605.
51 M. C. Alvarado, Recent progress in PVA/nanocellulose composite films for packaging applications: a comprehensive review, *Food Bioeng.*, 2024, **3**, 189–209.
52 F. Yudhanto, V. Yudha, H. S. B. Rochardjo, C. Budiyantoro, A. Khan, A. M. Asiri, *et al.*, Physical, mechanical and thermal properties of PVA/nanocrystalline cellulose bioplastic film, *Int. J. Eng., Trans. A*, 2024, **37**, 94–103.
53 N. Graupner, A. S. Herrmann and J. Müssig, Natural and man-made cellulose fibre-reinforced PLA composites: an overview, *Composites, Part A*, 2009, **40**, 810–821.
54 J. Lange and Y. Wyser, Recent innovations in barrier technologies for plastic packaging: a review, *Packag. Technol. Sci.*, 2003, **16**, 149–158.
55 M. C. Maes, W. Luyten, G. Herremans, R. Peeters, R. Carleer and M. Buntinx, Recent updates on EVOH barrier properties: a review, *Polym. Rev.*, 2018, **58**, 209–246.
56 A. V. García, N. J. Serrano, A. B. Sanahuja and M. C. Garrigós, Novel antioxidant packaging films based on PCL and almond skin extract, *Antioxidants*, 2020, **9**, 629.
57 N. Zhang, Y. Li, S. Wen, Y. Sun, J. Chen, Y. Gao, *et al.*, Analytical methods for determining peroxide value of edible oils: a mini-review, *Food Chem.*, 2021, **358**, 129834.
58 R. Melhaoui, S. Kodad, N. Houmy, K. Belhaj, F. Mansouri, M. Abid, *et al.*, Characterization of sweet almond oil content of European cultivars, *Scientifica*, 2021, **2021**, 9141695.
59 A. R. Sidhu, S. Naz, S. A. Mahesar, A. A. Kandhro, A. R. Khaskheli, Z. Ali, *et al.*, Effect of storage temperature on almond oil stability, *Food Mater. Res.*, 2023, **3**, 30.
60 B. M. Gracia, D. L. Reig, M. J. Rubio-Cabetas and M. A. García, Phenolic compounds and antioxidant capacity of Spanish almonds, *Foods*, 2021, **10**, 2334.
61 A. Valdés, C. Garrigós and A. Jiménez, Extraction and Characterization of Antioxidant Compounds in Almond (Prunus amygdalus) Shell Residues for Food Packaging Applications, *Membranes*, 2022, **12**, 806.
62 M. Farooq, E. Azadfar, A. Rusu, M. Trif, M. K. Poushi, Y. Wang, *et al.*, Improving the Shelf Life of Peeled Fresh Almond Kernels by Edible Coating with Mastic Gum, *Coatings*, 2021, **11**, 618.
63 A. J. Dijkstra, Vegetable Oils: Composition and Analysis, in *Encyclopedia of Food and Health*, Elsevier Inc., 2015, pp. 357–364.
64 P. Song, C. Chen, Q. Tian, M. Lin, H. Huang and S. Li, Two-stage oxygen supply strategy for enhanced lipase production by Bacillus subtilis based on metabolic flux analysis, *Biochem. Eng. J.*, 2013, **71**, 1–10.
65 M. Keramat, M. T. Golmakani, M. Aminlari and S. Shekarforoush, Oxidative Stability of Virgin Olive Oil Supplemented with Zataria multiflora Boiss. and Rosmarinus officinalis L. Essential Oils During Accelerated Storage, *J. Food Process. Preserv.*, 2017, **41**, e12951.
66 S. Cong, W. Dong, J. Zhao, R. Hu, Y. Long, X. Chi, *et al.*, Characterization of the lipid oxidation process of robusta green coffee beans and shelf life prediction during accelerated storage, *Molecules*, 2020, **25**, 1157.
67 S. El Bernoussi, I. Boujemaa, H. Harhar, W. Belmaghraoui, B. Matthäus, M. Tabyaoui, *et al.*, Evaluation of oxidative stability of sweet and bitter almond oils under accelerated storage conditions, *J. Stored Prod. Res.*, 2020, **88**, 10162.

